Received April 1998
Revised March 1999
Accepted April 1999

Finite element simulation of transient natural convection of low-Prandtl-number fluids in heated cavity

Habib Sammouda and Ali Belghith
Department of Physics,
Faculty of Sciences of Tunis, Tunis, Tunisia, and
Claude Surry
CNRS. Inst. of Sciences and of Genius Mat. Process,
Odeillo Font-Romeu, France

Keywords *Natural convection, Finite element, Heat, Fluid*

Abstract *The aim of the present investigation was to study numerically the transient of thermal convection in a square cavity filled with low-Prandtl-number fluids. The flow is driven by the horizontal temperature gradient between the vertical walls maintained at different temperatures. Two-dimensional equations of conservation and energy are solved using a finite element method and a fractional step time. The discrete equations systems are solved in the lap of each element-mesh with the aim of verifying the Boussinesq hypothesis locally. To compare our results with the earlier predictions, we have chosen the fluids for Prandtl-numbers 0.001, 0.005 and 0.01 and with Grashof numbers up to* 1×10^7*. To predict the steady state solutions with an oscillary transient period, the results are reduced in terms of the time series average Nusselt-number at the vertical walls, the velocity at the center of the cavity and near right boundary. In addition, the isotherms and the velocity field are produced with the aim of showing the main circulation and particularly the weak circulations at the corners of the cavity.*

1. Introduction

The convection due to thermal buoyancy force, in heated cavities, is an important and often dominant mode of heat and mass transport when the fluid is subjected to horizontal temperature gradient. Its dependence on geometry, Prandtl number (Pr), and Grashof number (Gr) is of practical importance in a number of heat transfer, materials processing, and other applications (Davis, 1983; Gebhart *et al.*, 1988).

The low-Prandtl number fluids are not much studied experimentally and particularly the flow due to thermal buoyancy force. The experimental diagnostic techniques, for these fluids, may introduce significant errors due to non-wetting between the fluid and the measuring probe. Flow visualisation is not possible owing to the opaqueness of these fluids and the use of radiation tracers is difficult. However, we refer to some papers (Yang, 1988; Palucci and Chenoweth, 1989; Stewart and Weinberg, 1972) where they have simulated a transient thermal convection using a variety of methods and particularly for cavities of large aspect ratio. Numerical predictions of steady state thermal convection in low-Prandtl number fluids have been made by different authors.

International Journal of Numerical Methods for Heat & Fluid Flow, Vol. 9 No. 5, 1999, pp. 612-624.

The interesting observation from the results of Steward and Weinberg (1972) is that the streamlines are almost square for high-Prandtl-number (Pr = 10) fluids, while they are almost circular for low-Prandtl-number (Pr = 0.013) flows.

Some results of these works are inconsistent. They have not taken into account the variation of physics properties of fluids due to convection phenomenon and its effect on the stability of flow. In effect, the stability of the various flow regimes and transitions between them has important consequences for the relevant technological processes.

Cless and Prescott (1996a, 1996b) have extended the study of Mohamad and Viskanta (1991) who compared the ability of different time marching schemes to resolved dynamical (oscillatory) behavior with the aim of improving the results. But we think that the ability of all numerical models used for these fluids is limited by the effecting of physical properties by the convection phenomenon such as the property of solidified material. For example, the convection is responsible for the formation of equiaxed grains, which is often desired, but it is also linked to a defect known as macrosegregation. Therefore, the Boussinesq approximation is not valid in the mass and it does not take into account this constraint by any models used in the literature.

In this direction, we propose in this study to use a finite element method for discretization in space. The elementary characteristic of this method allows us to verify the Boussinesq hypothesis locally. In addition, we use a fractional step for discretization in time to surmount the non-linearity of advection term and to diminish the effect of time marching scheme. The evolution in time of velocity and of Nusselt number allows us to detect when and for which value of Grashof number the steady state solution was achieved. Thus, we attempt to refine the critical Grashof number by predicting the periodic and oscillatory states for three fluids of low-Prandtl-numbers in order to exhibit also the effect of Prandtl-number on flow structures and on the onset of instability.

2. Problem formulation

We are concerned with the problem of fluids flow in a square cavity described in non-dimensional terms by $0 \leq x_1 \leq 1$ and $0 \leq x_2 \leq A$ with $A = \frac{H}{L}$ the aspect ratio, L and H are the length and height of cavity. The cavity has constant temperature on the vertical walls, T_1 on the hot wall and T_2 on the cooler wall, and has insulated horizontal walls (Figure 1). We shall consider the two-dimensional of transient viscous incompressible flow of fluids. The convective flow is generated by the buoyancy force as soon as $T_1 \neq T_2$ and its intensity depends on the magnitude of the temperature difference $\triangle T = T_1 - T_2$. Otherwise, here the flow is highly non-linear because the inertial force dominates the flow and the viscous effects are mainly confined to the boundary layers. For these reasons, we have chosen the convective-velocity $\sqrt{g\beta\Delta TL}$ as scale for velocity so that Gr = Re^2 and accordingly the advection terms are not too small compared with diffusive terms. Scales of L, ΔT, and $\frac{L}{\sqrt{g\beta\Delta TL}}$ are used for length, temperature and time respectively.

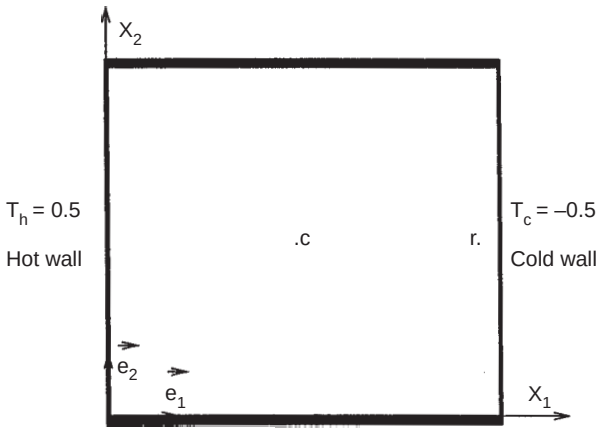

Figure 1.
Schematic diagram and coordinate system of the cavity

The set of dimensionless governing equations is then:

$$\frac{\partial \vec{u}}{\partial t} + (\vec{u}.\vec{\nabla})\vec{u} - \frac{1}{Re}\nabla^2\vec{u} + \frac{Gr}{Re^2}T\vec{x_2} + \vec{\nabla}p = \vec{0} \tag{1}$$

$$\vec{\nabla}.\vec{u} = 0 \tag{2}$$

$$\frac{\partial T}{\partial t} + (\vec{u}.\vec{\nabla})T - \frac{1}{RePr}\nabla^2 T = 0 \tag{3}$$

$\vec{u}$, p and T are the velocity, pressure and temperature fields respectively. Re, Gr and Pr are the classical Reynolds, Grashof and Prandtl numbers respectively. $\vec{\nabla}$ and ∇^2 are the gradient and Laplacian operators respectively.

The system of equations (1-3) is solved with suitable boundary conditions:

$$T = 0.5 \quad \text{at} \quad x_1 = 0 \tag{4}$$

$$T = -0.5 \quad \text{at} \quad x_1 = 1 \tag{5}$$

$$\frac{\partial T}{\partial x_2} = 0 \quad \text{at} \quad x_2 = 0, A = 1 \tag{6}$$

$$\vec{u} = \vec{0} \quad \text{at all boundaries.} \tag{7}$$

3. Basis of the numerical method

Various methods have been used to solve the system of equations (1-3). Finite difference, finite element and spectral methods have been employed using either stream function-velocity or primitive variable approaches. Our idea is to use a fractional step-time scheme for discretization in time (Jackson and Winters, 1984) with a semi-implicit type for a truncation error O ($\triangle t^2$), and a finite element method (Girault and Raviart, 1986) for discretization in space for

primitive variables. Then we surmount the non-linearity of advection term and we uncouple the convective and diffusive phenomena. Thus, the initial equations system is decomposed in the series of diffusive and convective steps where the local equations are obtained from the time t through the three time-steps $t + \frac{\triangle t}{3}$, $t + \frac{2\triangle t}{3}$ and $t + 1$, as follows:

(1) Step 1: step of diffusion with null divergence

$$\frac{2}{\triangle t}\vec{u}^{n+\frac{1}{3}} - \frac{2}{3Re}\nabla^2\vec{u}^{n+\frac{1}{3}} + \vec{\nabla}p^{n+\frac{1}{3}} = \frac{2}{\triangle t}\vec{u}^{n} + \frac{1}{3Re}\nabla^2\vec{u}^{n}$$

$$- \frac{Gr}{Re^2}T^n\vec{x}_2 - (\vec{u}^n.\vec{\nabla})\vec{u}^n \tag{8}$$

$$\vec{\nabla}.\vec{u}^{n+\frac{1}{3}} = 0 \tag{9}$$

$$\frac{2}{\triangle t}T^{n+\frac{1}{3}} - \frac{2}{3RePr}\nabla^2 T^{n+\frac{1}{3}} = \frac{2}{\triangle t}T^n + \frac{1}{3RePr}\nabla^2 T^n - (\vec{u}^n.\vec{\nabla})T^n \tag{10}$$

(2) Step 2: step of convection

$$\frac{1}{\triangle t}\vec{u}^{n+\frac{2}{3}} - \frac{1}{3Re}\nabla^2\vec{u}^{n+\frac{2}{3}} + (\vec{u}^{n+\frac{1}{3}}.\vec{\nabla})\vec{u}^{n+\frac{2}{3}} = -\vec{\nabla}p^{n+\frac{1}{3}} + \frac{1}{\triangle t}\vec{u}^{n+\frac{1}{3}}$$

$$+ \frac{2}{3Re}\nabla^2\vec{u}^{n+\frac{1}{3}} - \frac{Gr}{Re^2}T^{n+\frac{1}{3}}\vec{x}_2 \tag{11}$$

$$\frac{1}{\triangle t}T^{n+\frac{2}{3}} - \frac{1}{3RePr}\nabla^2 T^{n+\frac{2}{3}} + (\vec{u}^{n+\frac{1}{3}}.\vec{\nabla})T^{n+\frac{2}{3}} = \frac{1}{\triangle t}T^{n+\frac{1}{3}}$$

$$+ \frac{2}{3RePr}\nabla^2 T^{n+\frac{1}{3}} \tag{12}$$

(3) Step 3: second step of diffusion with null divergence

$$\frac{2}{\triangle t}\vec{u}^{n+1} - \frac{2}{3Re}\nabla^2\vec{u}^{n+1} + \vec{\nabla}p^{n+1} = \frac{2}{\triangle t}\vec{u}^{n+\frac{2}{3}} + \frac{1}{3Re}\nabla^2\vec{u}^{n+\frac{2}{3}}$$

$$+ \frac{Gr}{Re^2}(\frac{-1}{3}T^{n+\frac{1}{3}} + \frac{4}{3}T^{n+\frac{2}{3}})\vec{x}_2 + (\frac{1}{3}\vec{u}^{n+\frac{1}{3}}.\vec{\nabla} - \frac{4}{3}\vec{u}^{n+\frac{2}{3}}.\vec{\nabla})\vec{u}^{n+\frac{2}{3}} \tag{13}$$

$$\vec{u}^{n+\frac{2}{3}} = 0 \tag{14}$$

$$\frac{2}{\triangle t}T^{n+1} - \frac{2}{3RePr}\nabla^2 T^{n+1} = \frac{2}{\triangle t}T^{n+\frac{2}{3}} + \frac{1}{3RePr}\nabla^2 T^{n+\frac{2}{3}}$$

$$+(\frac{1}{3}\vec{u}^{n+\frac{1}{3}} - \frac{4}{3}\vec{u}^{n+\frac{2}{3}}).\vec{\nabla}T^{n+\frac{2}{3}} \qquad (15)$$

In steps 1 and 3 the velocity and pressure fields are solutions of generalized Stokes problem. The advection and buoyancy force terms are in explicit form. In step 2 the advection term is semi-implicit. The temperature field in different steps and the velocity field in advection step verify the linear and decoupled equations, so the discrete spatial approximation will be directly applied.

The generalized Stokes-problem can be written as follows:

$$\begin{cases} \alpha\vec{u} - \nu\nabla^2\vec{u} + \vec{\nabla}p = \vec{f} \\ \vec{\nabla}.\vec{u} = 0 \quad \text{on the domain of calcul}\Omega \\ \vec{u} = \vec{0} \quad \text{on} \quad \partial\Omega = \Gamma \\ \text{with} \quad \alpha = \dfrac{2}{\triangle t} \quad \text{and} \quad \nu = \dfrac{2}{3Re} \end{cases}$$

We have chosen a continuous quadrilateral element of high precision with a quadratic interpolation Q2 for a velocity and a bilinear one Q1 for the pressure as shown in Figure 2. This combination of interpolation for velocity-pressure (Q2-Q1) gives a stable scheme that verifies the Babûska-Brezzi condition (Girault and Raviart, 1986). The temperature is approached by the quadratic element Q2 as velocity.

To overcome the constraint of non-validation of Boussinesq hypothesis to global scale, we have proceeded to solve the discrete equations systems to elementary scale where the physical properties are constant in each element-mesh. In effect, the use of continuous and conformable elements allows us to write the global system equations as an assembly of elementary systems (Hughes, 1988). Then, the element vectors of nodal pressures and nodal velocities are determined by solving the elementary systems. In addition, with this procedure we exclude all instability of flow due to the variation of physical

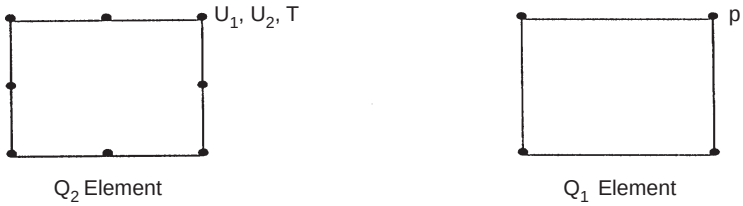

Figure 2.
Schematic diagram of quadratic element (Q2) and of bilinear element (Q1)

properties. The conjugate gradient method founded on the Uzawa algorithm and the preconditioner of Cahouet and Chabart (1988) are used to solve the discrete equations systems and to close the pressure operator.

All the calculation began with a stagnant fluid, and the temperature of the left vertical wall was suddenly increased to a constant value for $t \geq 0$. Preliminary calculations were also performed using 51×51, 41×41, 31×31 and 21×21 grids, but the time-average Nusselt numbers differed by less than 0.5 percent from one case to another. Furthermore, the period of oscillation was predicted to be the same for the four grids. It is assumed that the uniform 21×21 mesh is sufficiently fine owing to the high precision of the quadratic element Q2 used for interpolation of the velocity and the temperature. In effect, each mesh is approached by an element with eight nodes where the velocity and the temperature are calculated at each of these nodes. To compare this with the results of Mohamad and Viskanta (1991)[9] where, with a finite difference method, 61×61 and 81×81 meshes are chosen, as grid independent of results and where the velocity and temperature are calculated at the midpoint of each mesh, our uniform grid is considered independent of the results.

Time steps of 0.01 and 0.001 were tested for the same Prandlt and Grashof numbers, and the results were found to be consistent without difference between the two cases. We have opted to carry all calculations with the step 0.01 owing to the fractional step-time method used where the step-time is divided, once more, in two by construction of moment and energy equations in each step.

4. Results and discussion

For convenience reasons to compare with earlier results, we have chosen three fluids for low-Prandtl-number 0.001, 0.005 and 0.01. Otherwise, the critical values of Grashof number, given by some authors, are served for our analysis as a starting point to search the accurate threshold values.

Results for Pr = 0.001

For Prandtl number Pr = 0.001 and Grashof number $Gr = 9 \times 10^5$ no oscillation or circulation in cavity corners was predicted. This proves that flow and temperature fields gradually approached steady state. When the Grashof number increases to 1×10^6, oscillatory flow is started with a very low frequency as shown in Figure 3a in the variation, with time, of the U_1-velocity at the center of the cavity. The average Nusselt number at both vertical walls of the cavity ($x_1 = 0$ or $x_1 = 1$) increased slowly without convergence (Figure 3b). Velocity field revealed one main circulation (Figure 3c) without circulation in cavity corners.

For $Gr = 2 \times 10^6$ the oscillatory transient period was followed by an oscillating flow (Figure 3d). The computation is extended for long periods of time to predict the attitude of the oscillations. We remark that after t = 11.5 the oscillations are amplified and periodic flow is established. The Nusselt number

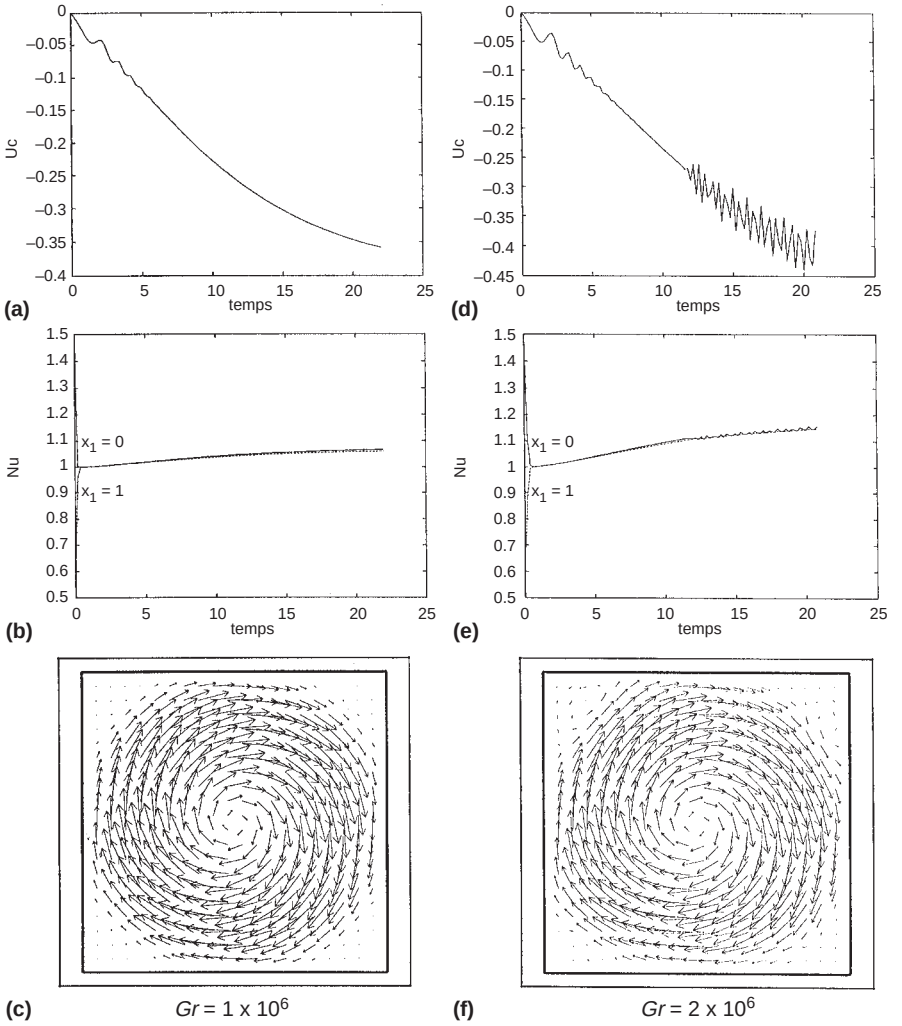

Figure 3.
Time series of U_1-velocity at the center of the cavity, of the average Nusselt number at both vertical walls and of velocity field for Pr = 0.001; and for Gr = 1×10^6 (a,b,c) and for Gr = 2×10^6 (d,e,f)

did not show convergence but increases with oscillations of feeble amplitude (Figure 3e). The velocity field revealed one main circulation with some circulations in the superior corners (Figure 3f).

For Gr = 3×10^6 the periodic flow is predicted. This is displayed for the U_1-velocity (Figures 4a, 4b) at the center of the cavity and at the mid-cavity near the right boundary (as located in Figure 1). It should be noticed that all the locations in the cavity revealed similar trends and differed only in amplitude.

Thus, the damped oscillatory transient periods were predicted for Gr = 1×10^6 and the periodic flow at Gr = 3×10^6, while the results of Mohamad and Viskanta (1991) revealed these phenomena at Gr = 2×10^6 and at Gr = 3×10^6 respectively.

Results for Pr = 0.005

For Pr = 0.005 and Gr = 9×10^5 the flow and temperature fields approach a steady state solution. In effect, the time series for U_1-velocity showed uniform evolution without any oscillation. However, the results for Gr = 1×10^6 reveal that the velocity field is almost circular in shape with one main circulation and any others are present at the cavity corners (Figure 5c). The time history of the velocity field reveals decaying oscillations transient that are dumped after a short time (Figure 5a).The duration of the transient stage needed to reach steady state is t = 6. The average Nusselt numbers at both vertical walls of the cavity converge to 1.5236 (Figure 5b).

For Gr = 2×10^6, the Figures 5d, 5e, and 5f reveal decaying oscillations for the U_1-velocity time evolution and show that the Nusselt number increases slowly but it does not converge and some weak circulations in corners begin to appear.

For Gr = 3×10^6, the flow field at the center of cavity oscillates with a dimensionless frequency ($\frac{1}{t}$ = 1.6) (Figure 6a) and the Nusselt-number converges to about the value 2.000 with oscillations of feeble amplitude (Figure 6b). Otherwise, the corner circulations are cleanly established. The identical phenomena are noticed for Gr = 5×10^6 where we have performed the computations for long periods of time during which the solution behaviour remained unchanged. Moreover, if we compare in Figure 7 the variation in time of velocity respectively for Gr = 1×10^7 and Gr = 5×10^6, we notice that the frequency of oscillations decreases where Gr increases for the same Prandtl number 0.005.

It should be mentioned that Mohamad and Viskanta (1991) predicted oscillatory flow for Pr = 0.005 at Gr $> 3 \times 10^6$ and Benocci (1983) at Gr = 1×10^7 whereas our results reveal oscillating flow for Gr $> 1 \times 10^6$.

Results for Pr = 0.01

For Pr = 0.01 and Gr = 1×10^7, the velocity field reveals two rotating cells of same direction inside the one main circulation limited by the lateral confinement. In addition, the cells are cleanly developed in the four corners of

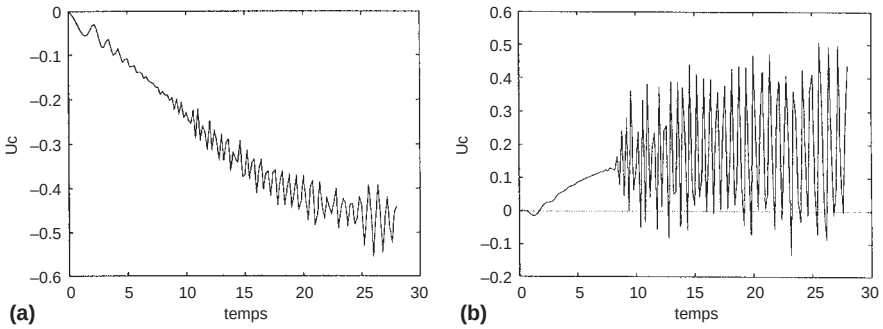

Figure 4.
Time series of U_1-velocity at the center of the cavity (a) and at the mid-cavity near the right boundary (b) for Pr = 0.001 and Gr = 3×10^6

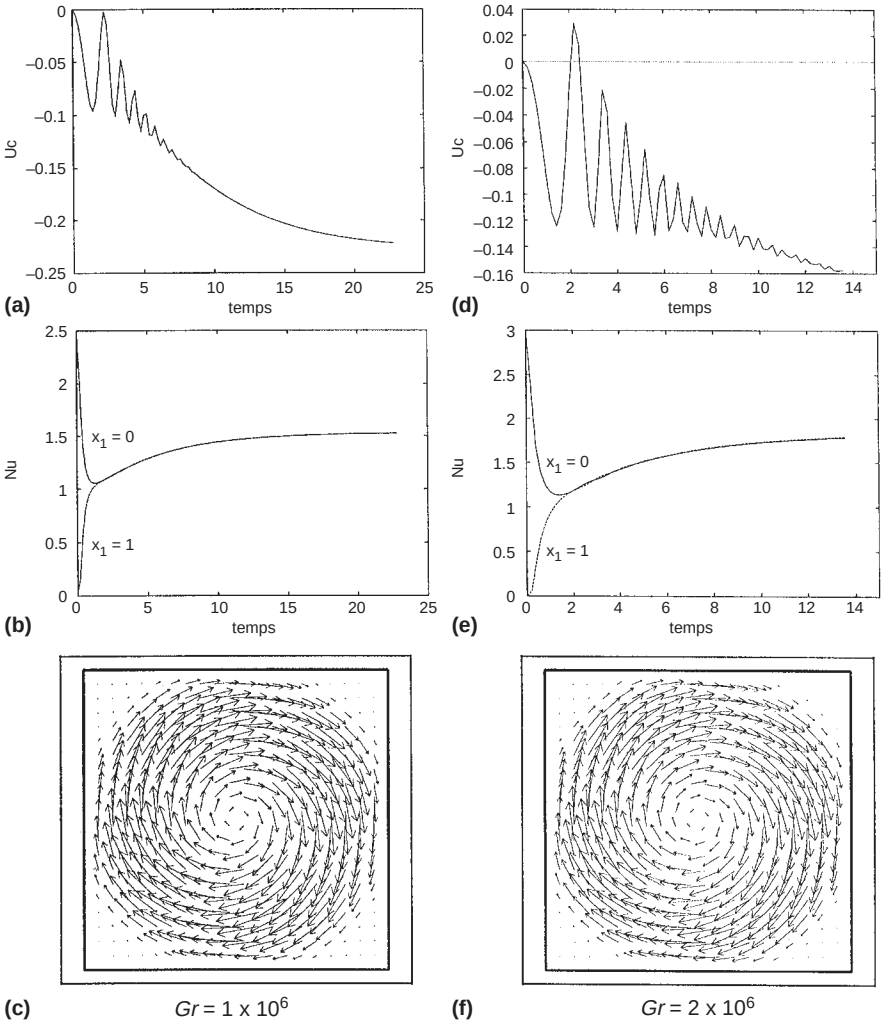

Figure 5.
Time series of U_1-velocity at the center of the cavity and of the average Nusselt number at both vertical walls and of velocity field for Pr = 0.005; and for Gr = 1×10^6 (a,b,c) and for Gr = 2×10^6 (d,e,f)

the cavity and in the time series of the U_1-velocity at the center (Figures 8a, 8b). Results of Mohamad and Viskanta (1991) have predicted similar phenomena.

If we decrease the Grashof number to 8×10^6 and to 5×10^6, we predict a periodic flow. The principal frequencies ($\frac{1}{t}$) are 1.1 and 1.3 respectively. Gresho and Upson (1983), using 70×70 uniform elements meshes, predicted similar phenomena.

However, for Gr = 4×10^6 the oscillations begin to decay without dump after a long period of time as shown in Figure 9a. Figure 9b shows the growth of Nusselt-number for both vertical walls with oscillations of feeble amplitude without convergence. Identical phenomena are predicted for Gr = 3×10^6 and Gr = 2×10^6.

For Gr = 1×10^6 a decaying oscillatory transient was predicted and they are dumped after a short time (Figure 10a) and the velocity field is almost circular in shape with one main circulation and any one is present at the cavity corners (Figure 10b). Therefore, the critical value of Grashof number is Gr = 9×10^5 where no oscillation was predicted and the flow field asymptotically approaches a steady state.

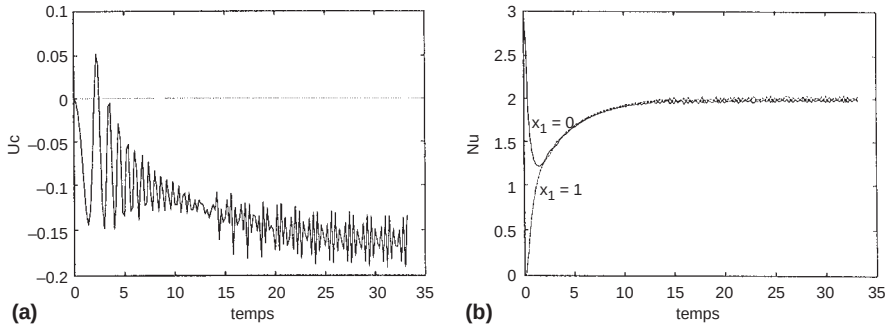

Figure 6.
Time series of U_1-velocity at the center of the cavity (a) and of the average Nusselt number at both vertical walls (b) for Pr = 0.005 and Gr = 3×10^6

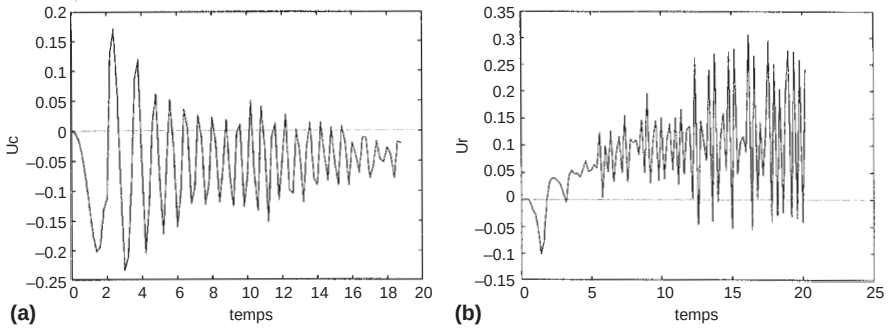

Figure 7.
Time series of U_1-velocity at the center of the cavity for Pr = 0.005 and for Gr = 1×10^7 (a) and Gr = 5×10^6 (b)

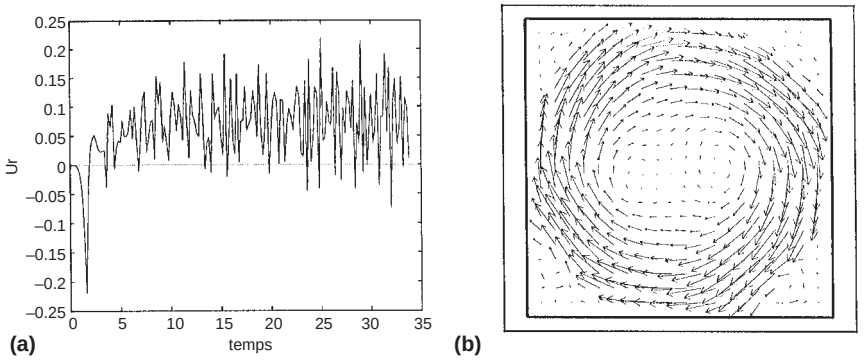

Figure 8.
Time series of U_1-velocity at the center of the cavity (a) and velocity field (1cm = 1.521) at t = 25.2 for Pr = 0.01 and Gr = 1×10^7

Comparison of results

Table I summarizes the results of the predictions given by our study and that of Mohamad and Viskanta (1991). We noticed that the critical values are different for the two studies. Otherwise, a comparison of these results shows that the steady state flow and the decaying oscillatory transient are predicted, for all fluids of Prandtl-numbers 0.001, 0.005 and 0.01, almost at identical values of Grashof-numbers $Gr = 9\times10^5$ and $Gr = 1\times10^6$ respectively, but the critical values for periodic regimes are different for three fluids. We noticed

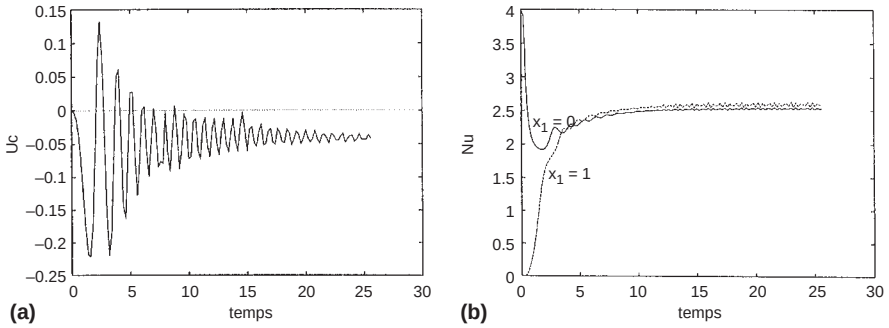

Figure 9.
Time series of U_1-velocity at the center of the cavity (a) and of the average-Nusselt at both vertical walls (b) Pr = 0.01 and Gr = 4 $\times10^6$

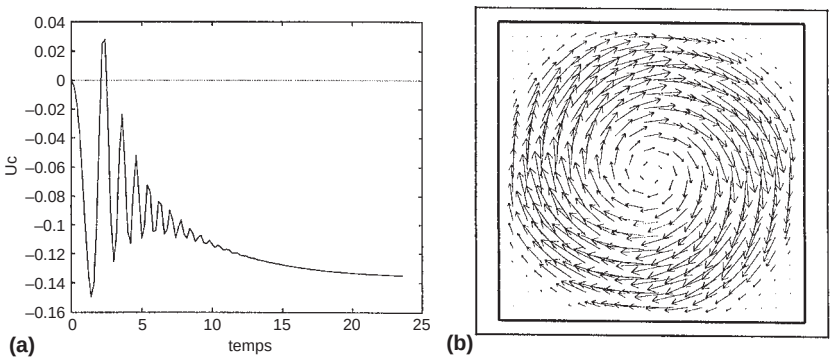

Figure 10.
Time series of U_1-velocity at the center of the cavity (a) and the velocity field (b) for Pr = 0.01 and Gr = 1 $\times10^6$

Pr	Results	Steady states	Dumped oscillations	Periodic flow	Dimensionless frequency
0.001	Our results	9×10^5	1×10^6	3×10^6	1.4
	Mohamad and Viskanta (1991)	1×10^6	2×10^6	3×10^6	
0.005	Our results	9×10^5	1×10^6	3×10^6	2.4
	Mohamad and Viskanta (1991)	1×10^6	3×10^6	5×10^6	1.0
0.01	Our results	9×10^5	1×10^6	5×10^6	3.1
	Mohamad and Viskanta (1991)	3×10^6	5×10^6	8×10^6	

Table I.
Summary of numerical results

also, that as the Prandtl-number increases the period of oscillation transient regime decreases, as mentioned by Mohamad and Viskanta (1991).

It should be mentioned that the improvement of results noticed relative to that of Mohamad and Viskanta (1991) is due to several factors. The first factor is the use, in our study, of convective velocity as reference velocity. In effect, its advantage is that the increase of Grashof number induces the effect of diffusive term in moment and energy equations, and in consequence the thickness of dynamic and thermical boundary layers reduces the ability to explore fully the zones near walls. The second factor is the conception of a numerical model so that diffusive and convective phenomena are separated in three steps, allowing a diminution of the effect of non-linearity on the stability of the numerical scheme. The third factor is the validity of the Boussinesq hypothesis allowing the elimination of the flow instability due to the variation of fluid physical properties.

Thus, we have attempted to eliminate all factors responsible for instability conditions. In effect, for aspect ratio A = 4 and Pr = 0.015, Winters (1987) has used a technique which locates hopf bifurcation condition and he predicted a threshold value $Gr = 5.91 \times 10^4$ for oscillatory convection, whereas Crochet *et al.* (1987), using direct simulation, predicted a value $Gr = 3.2 \times 10^5$ without specifying if it is the critical value.

Otherwise, this study shows that vorticity dynamics along the outer periphery and corners of the cavity were primarily responsible for oscillatory conditions. In effect, four weak circulation cells were predicted at the corners of the cavity. The strength of the upper left-hand and lower right-hand circulations. Our results showed that the upper right and lower left-hand corner vortices evolved first, followed by the vortices in the other two corners. This finding is consistent with the results of Gresho and Upson (1983) and that of Mohamad and Viskanta (1991). Accordingly, the accurate determination of the threshold of oscillatory convection by direct simulation is very delicate, because it depends strongly on the numerical method used, on the number of meshes and on the aspect ratio of cavity. Moreover, the lack of experiment results for low-Prandtl-number flows, for reasons above-mentioned, urges us to improve the numerical results by using numerical experimentation and adequate models.

5. Conclusion

In this paper, we have attempted to determine the accurate values of threshold of oscillatory convection in a square cavity (A = 1) differentially heated and filled with fluids of low-Prandtl-numbers Pr = 0.001, 0.05 and 0.01. The fractional step-time method and finite element method are used for the discretization of time and space respectively. A range of Grashof numbers up to 1×10^7 has been investigated. These results show that for $Gr = 9 \times 10^5$, the flow field asymptotically approaches steady state with Pr = 0.001, 0.005 and 0.01. Otherwise, for $Gr = 1 \times 10^6$, the dumped oscillatory transient periods were predicted for all considered Prandtl-numbers. Finally, periodic flow was

predicted for Pr = 0.001, 0.005 and 0.01 at Grashof numbers of 3×10^6, 3×10^6 and 5×10^6 respectively. To improve the previous results, we have attempted to eliminate all instability causes such as variation of physical properties (Boussinesq hypothesis), non-linearity of convective term and the effect of time marching numerical schemes. Thus, we have contributed to lower the spread found among the numerical results and the results of stability analysis, owing to the lack of experimental results of low-Prandtl-number flows.

References

Benocci, C. (1983), "Thermohydraulics of liquid metals: turbulence modeling in liquid metal free convection", *Von Karman Institute Lecture Series 1983-07*.

Cahouet, J. and Chabart, J.P. (1988), "Some fast 3D finite element solvers for the generalized Stokes problem", *Int. Jour. Num. Meth. Fluids*, Vol. 8, pp. 869-85.

Cless, C.M. and Prescott, P.J. (1996a), "Effect of time varying thermal boundary conditions on oscillatory natural convection of a low-Prandtl-number fluid", *Numerical Heat Transfer*, Part A, Vol. 29, pp. 645-69.

Cless, C.M. and Prescott, P.J. (1996b), "Effect of time marching schemes on predictions of oscillatory natural convection in fluids of low-Prandtl-number", *Numerical Heat Transfer*, Part A, Vol. 29, pp. 575-97.

Crochet, M.J., Geyling, F.T. and Van Schaftingen, J.J. (1987), "Numerical simulation of the horizontal Bridgman growth Part I: Two-dimensional flow", *Int. Jour. Num. Meth. Fluids*, Vol. 7, pp. 29-48.

Davis, G. De Vahl (1983), "Natural convection of air in a square cavity: a benchmark numerical solution", *Int. Jour. Num. Meth. Fluids*, Vol. 3, pp. 249-64.

Gebhart, B., Jaluria, Y., Mahajan, R.L. and Sammakia, B. (1988), *Buoyancy-Induced Flows and Transport*, Hemisphere, Washington, DC.

Girault, V. and Raviart, V.A. (1986), "Finite element methods for Navier Stokes equations", Springer Verlag.

Gresho, P.M. and Upson, C.G. (1983), "Application of a modified finite element method to the time-dependent thermal convection of a liquid metal", in Taylor, C., Johnson, C., Smith, J.A. and Ramsey, W. (Eds), *Proc. 3rd Int. Conf. on Numerical Methods in Laminar and Turbulent Flow*, Pineridge, Swansea, pp. 750-62.

Hughes, T.J.R. (1988), *Linear Static and Dynamic Finite Element Analysis*, Prentice-Hall Inc., Englewood Cliffs, NJ.

Jackson, C. and Winters, K.H. (1984), "A finite element study of the Benard problem using parameter stepping and bifurcation search", *Int. Jour. Num. Meth. Fluids*, Vol. 4, pp. 127-45.

Mohamad, A.A. and Viskanta, R. (1991), "Transient natural convection of low-Prandtl-number fluids in a differentially heated cavity", *Int. Jour. Num. Meth. Fluids*, Vol. 13, pp. 61-81.

Palucci, S. and Chenoweth, D.R. (1989), "Transition to chaos in a differentially heated vertical cavity", *J. Fluid Mech.*, Vol. 201, pp. 379-410.

Stewart, M.J. and Weinberg, F. (1972), "Fluid flow in liquid metals, I.Theoretical analysis", *J. Cryst. Growth*, Vol. 12, pp. 217-27.

Winters, K. (1987), "Oscillatory convection in crystal melts:the horizontal Bridgman process", Report TP-1230, Theoretical Physics Division, Harwell Laboratory.

Yang, K.T. (1988), "Transitions and bifurcations in laminar buoyant flows in confined enclosures", *Journal of Heat Transfer*, Vol. 110, pp. 1191-203.